

Supporting Information

Bio-inspired Nanofibrils-humped Fibers with Strong Capillary for Fog Capture

Yufang Liu,[†] Nan Yang,[‡] Chunlei Gao,[†] Xin Li,[†] Zhenyu Guo,[†] Yongping Hou^{*,†}, Yongmei Zheng^{*,†}

*[†]Key Laboratory of Bio-Inspired Smart Interfacial Science and Technology of Ministry of Education
School of Chemistry, and Beijing Advanced Innovation Center for Biomedical Engineering, Beihang
University (BUAA), Beijing 100191, P. R. China*

*[‡]Shanghai Electro-Mechanical Engineering Institute
Shanghai 201109(P. R. China)*

Email: huyongping09@buaa.edu.cn; zhengym@buaa.edu.cn

Contents:

Supplementary Figure Legends: Figure S1-S14

Supplementary analysis I - III

Supplementary Movies: Movie S1-S5

Supplementary Figures:

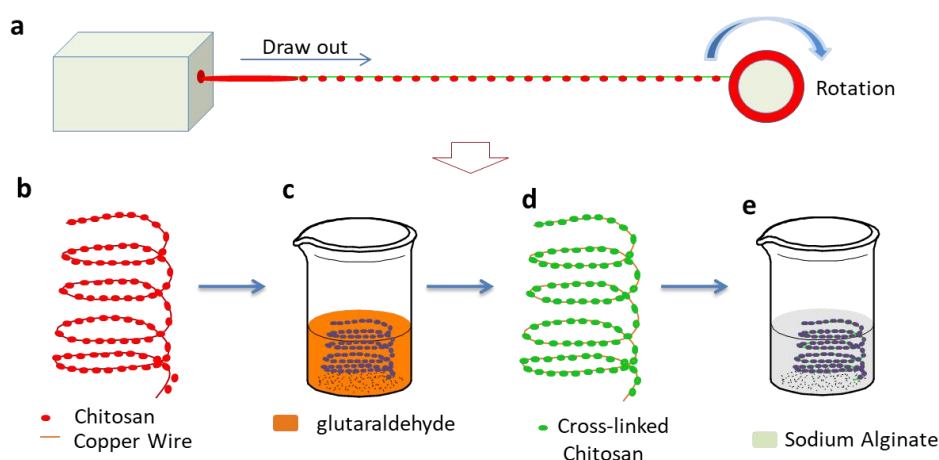


Figure S1. Illustration on fabrication of based-fiber with chitosan and sodium alginate spindle-knots (original spindle-knotted fiber) as electrospinning collector. **a)** Fluid-coating method for spindle-knots. Chitosan fluid is poured in a hollow container with two pinholes on two opposite sides. Copper wire is drawn out of the hollow container through the pinhole to obtain spindle-knot copper wire. **b-e)** Schematic of preparation process for based-fiber with chitosan and sodium alginate spindle-knots. In this process, the spindle-knot copper wire is dried and immersed into glutaraldehyde solution (10 wt.%) for 60 min to get cross-linked chitosan spindle-knot copper wire and dried at 75 °C. After that, cross-linked chitosan spindle-knot copper wire is immersed into sodium alginate solution (2 wt.%) for another 60 min and dried at 75 °C. Thus the based-fiber with chitosan and sodium alginate spindle-knots can be achieved as the electrospinning collector.



Figure S2. Optical images of water contact angle (CA) of a nanofibrils surface. The surface is covered by thermoplastic polyester elastomer (TPEE) and chitosan (CS) nanofibrils. **a)** Photographed at 0 s (CA=50 °). **b)** Photographed after 5 s (CA=30 °).

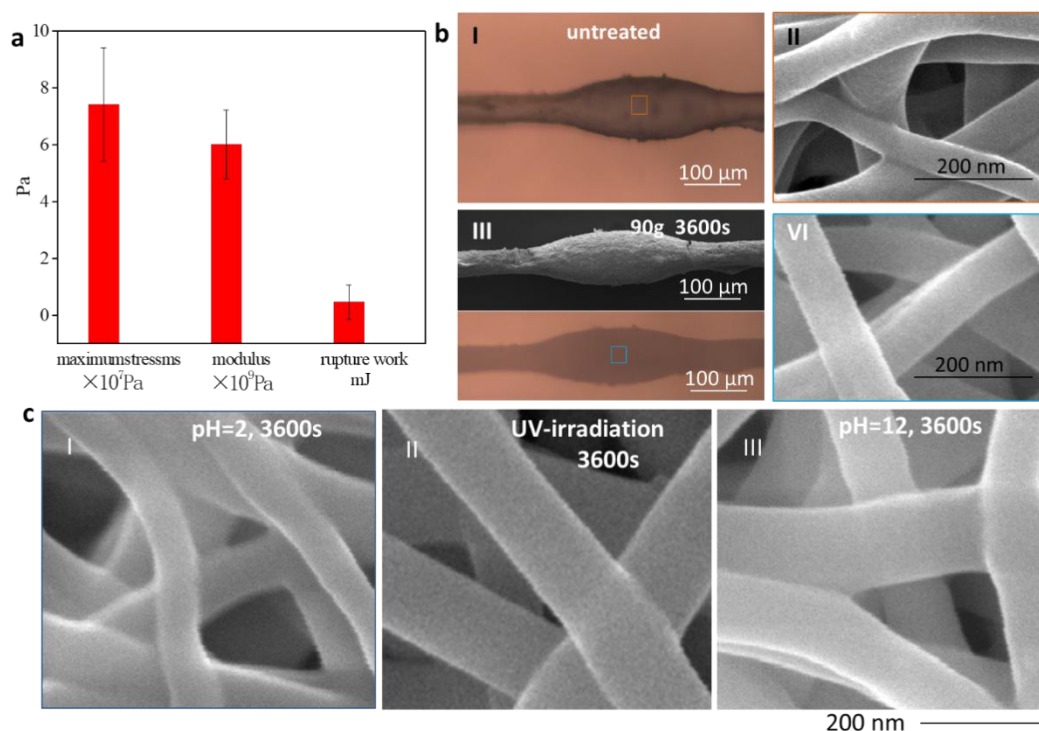


Figure S3. a) A plot of Young modulus, rupture work and maximum stress of BNF. There are maximum stress of 7.42×10^7 Pa, Young modulus of 6.02×10^9 Pa, and rupture work of 0.48 mJ, respectively. b) Optical images and SEM images of BNF before and after press with a 90g weight. There is no any change on microstructure. c) SEM images of acetic acid treated BNFs, alkali acid treated BNFs and BNF after UV irradiation 3600s. After suffering ultraviolet radiation (320-450 nm) for 3600 s, BNF exhibits excellent UV resistance ability and its surface features keep stable primarily.

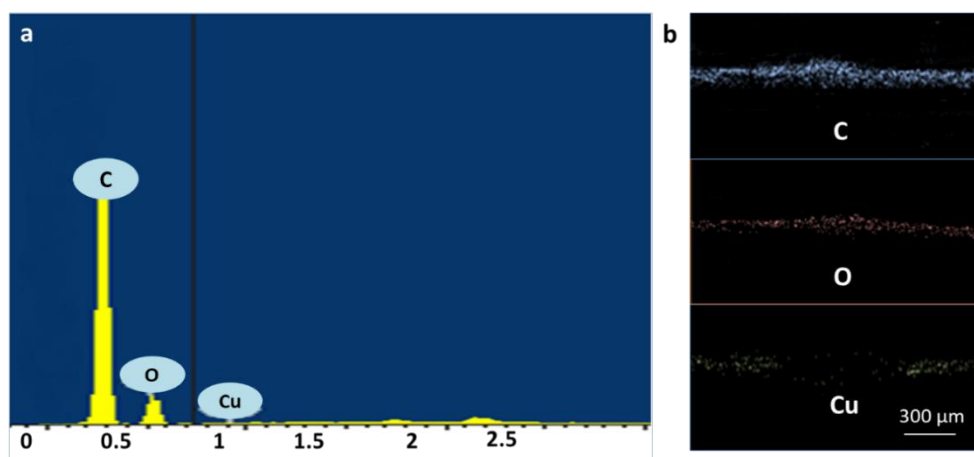


Figure S4. **a)** SEM images via EDS analysis on component elements of the BNF surface. **b)** EDS maps. C-, O-, and Cu-dominated elements are indicated with blue scatters (the upside), yellow scatters (the middle), green scatters (the below), respectively.

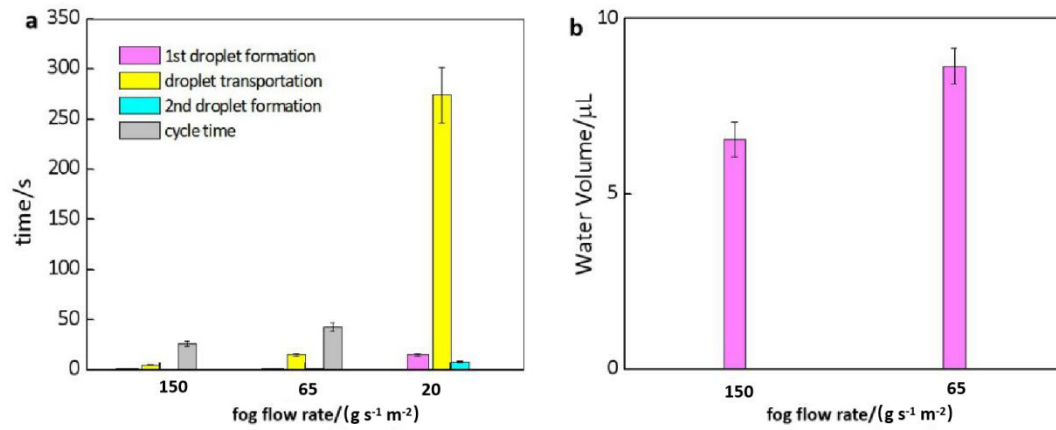


Figure S5 a) Fog harvest time of BNFs at fog flow rate of $150 \text{ g s}^{-1} \text{m}^{-2}$, $65 \text{ g s}^{-1} \text{m}^{-2}$, and $20 \text{ g s}^{-1} \text{m}^{-2}$, respectively. The fog harvest time of BNF increase with the fog flow rate decline (from $150 \text{ g s}^{-1} \text{m}^{-2}$, $65 \text{ g s}^{-1} \text{m}^{-2}$, and $20 \text{ g s}^{-1} \text{m}^{-2}$), such as first droplet formation time (1 s, 1.5 s, 15s), droplet transportation time (5 s, 15 s, 274 s), second droplets formation time (0.4 s, 0.8 s, 8 s) and cycle period increase (26 s, 43 s, more than 300 s), respectively. **b)** Maximum droplet volume of BNFs are $\sim 6.5 \mu\text{L}$ at $f= 150 \text{ g s}^{-1} \text{m}^{-2}$ and $8 \mu\text{L}$ at $f= 65 \text{ g s}^{-1} \text{m}^{-2}$.

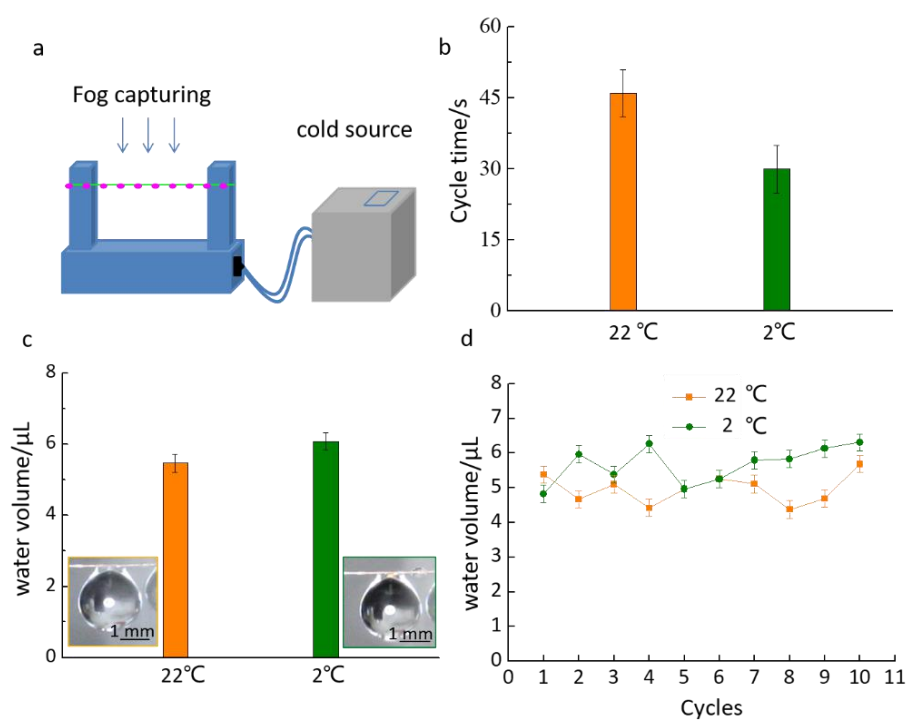


Figure S6. Water collection of BNF at different temperatures of 2°C and 22°C. **a)** Schematic of BNF fog capturing system. **b)** Cycle time in different temperature. The cycle time can be defined as the time that critical droplets detached off surface of BNFs from droplet capture. Fog-droplets collection cycle time at 22°C takes the time of 45 s, but take 30 s at 2°C. **c)** Compare on maximum droplet volume between both temperature. The water volume is larger at 2°C than that at 22°C. **d)** Compare on water volume versus cycle numbers. Due to the higher adhesion on BNF at 2 °C, the maximum hanging droplets volume is slightly bigger one, which is equal to 6 μL in 10 cycles.

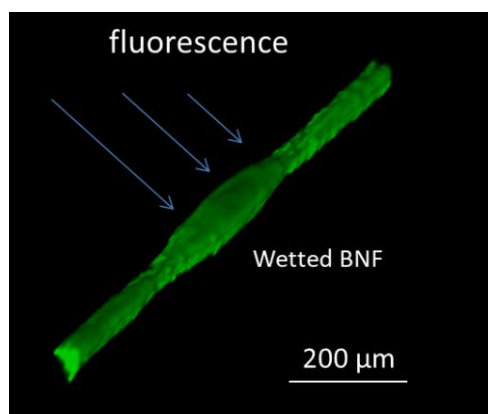


Figure S7. Confocal fluorescence image of wetted BNF. Water with trace amounts of fluorescein is nebulized by humidifier and collected by BNF to visualize the water film of BNF.

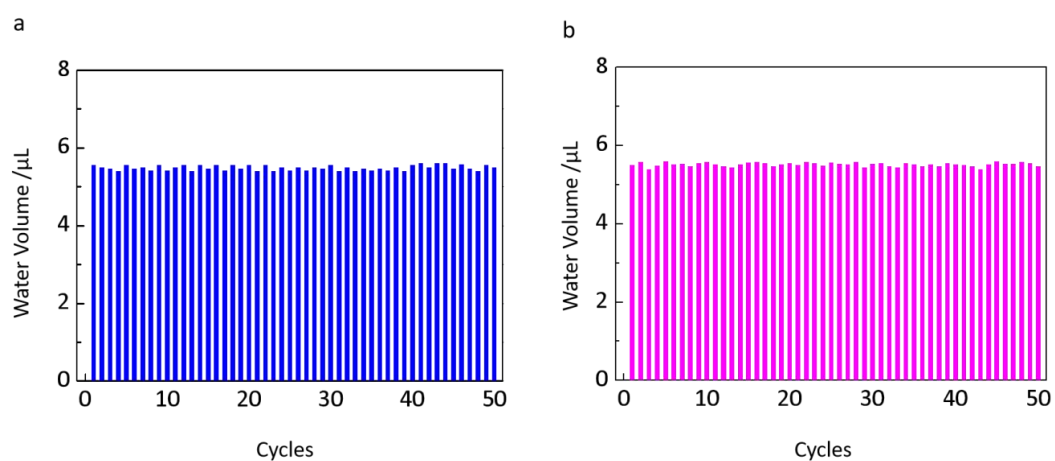


Figure S8. Stability of BNF for the maximum water volumes. a) In fifty water-collecting cycles. b) Stored for one month in fifty water-collecting cycles. The maximum hanging water volumes are kept to up to $\approx 5.5 \mu\text{L}$.

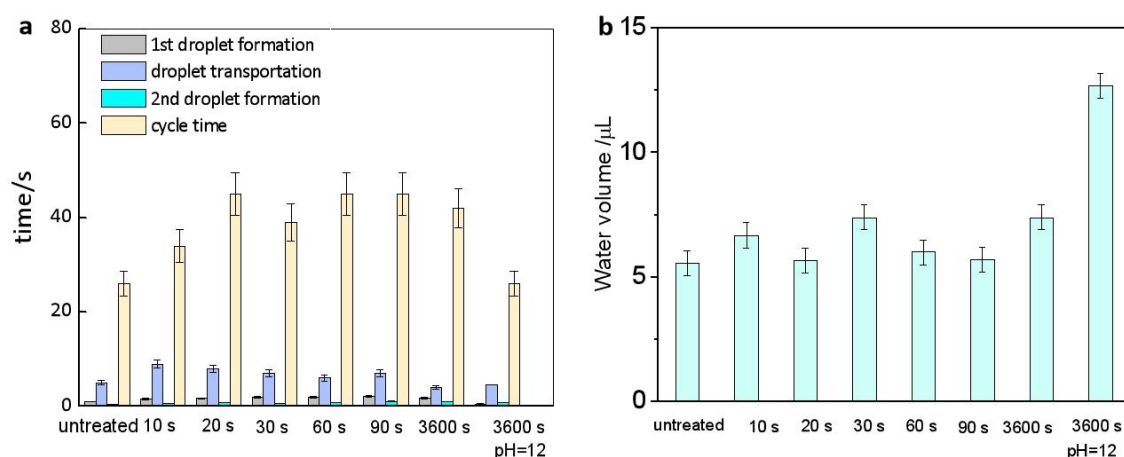


Figure S9. a) The fog collection processes of untreated, acetic acid treated (10, 20, 30, 60, 90, 3600 s), and alkali treated (NaOH, 3600 s) BNFs at fog flow rate (f) of $150 \text{ g s}^{-1} \text{ m}^{-2}$ were observed by naked eyes, respectively. This process are consisted of two cycles. At the first cycle, on the dry BNF, the first droplet arise (1st droplet formation) and droplet began transport. At the second cycle, the first droplet arise (2nd droplet formation), droplet began transport, and the cycle time. Compared with the untreated BNF, acid treated and alkali treated BNFs can still exhibit good water collection behavior. Furthermore, at the second cycle, the first droplet formation time (2nd droplet formation) is much shorter than that of the first cycle (1st droplet formation), which means the wetted BNF has higher collection efficiency on account of the inside transportation. **b)** Maximum droplet hanging volume of above-mentioned samples, in the same observation and testing condition.

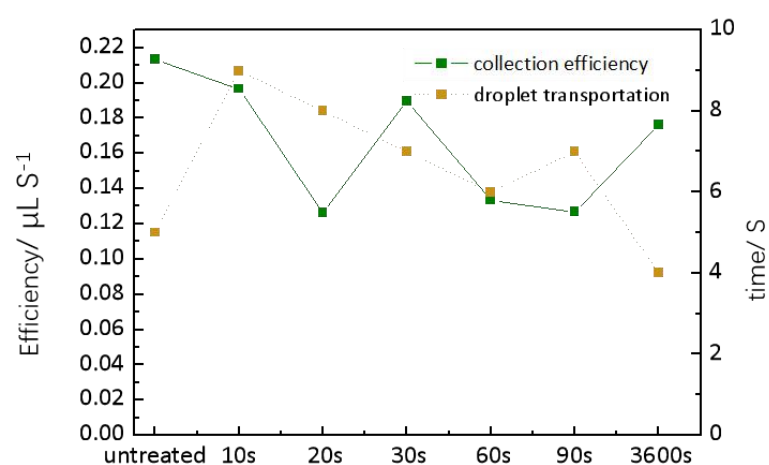


Figure S10. A plot of the water collection efficiency and droplet transportation time of untreated, acetic acid treated (10, 20, 30, 60, 90, 3600 s) BNFs, respectively, from which it is obvious to find out that longer droplets transportation time induce lower water collection efficiency.

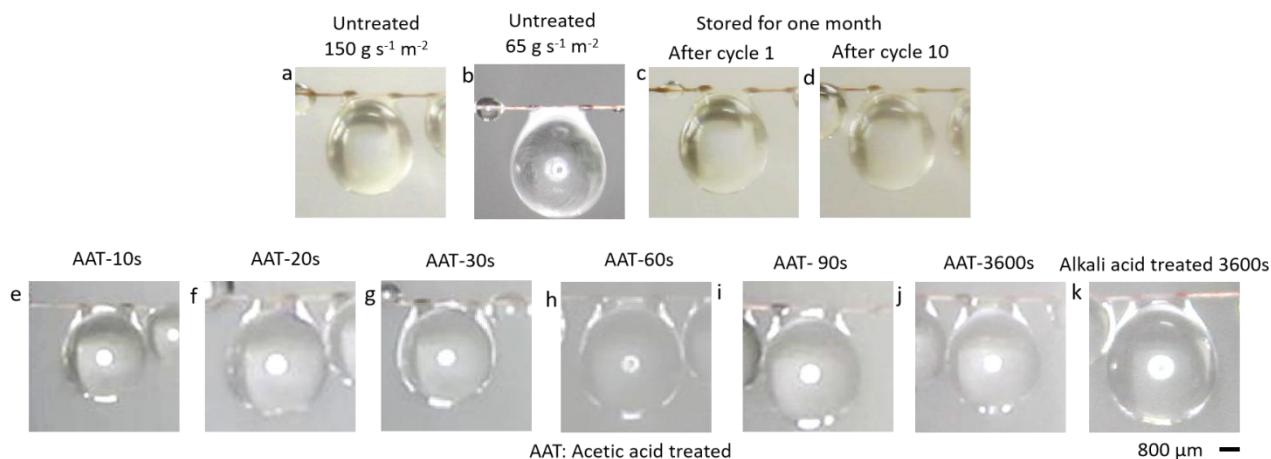


Figure S11. Optical images for maximum suspension droplets (critical droplets) on BNFs in different conditions: **a)** at fog flow rate of $150 \text{ g s}^{-1} \text{ m}^{-2}$. **b)** at fog flow rate of $65 \text{ g s}^{-1} \text{ m}^{-2}$. **c)** stored for one month in one water-collecting cycle. **d)** stored for one month in ten water-collecting cycles. **e-j)** acetic acid treatment (AAT) in different times of 10 s (e, AAT-10s), 20 s (f, AAT-20s), 30 s (g, AAT-30s), 60 s (h, AAT-60s), 90 s (i, AAT-90s), 3600 s (j, AAT-3600s). **k)** alkali acid treatment (e.g., NaOH) in 3600 s .

Supplementary analysis I:

To elucidate the mechanism, we consider there is the case of channel between nanofibrils, which would play a role for droplet transport. The main driving force in nanofibrils gaps of wetted BNF can be discussed. During water collection process, the wetted BNF can be viewed as a connected water column with several small water droplets at nanofibrils humps. Tiny droplets in mist connected with the water column as soon as captured on the wetted BNF and shrink by additional pressure. We suppose that horizontal nanofibrils channels of BNF is created by four adjacent nanofibrils, as shown in **Figure S12a**, which means the gravity is negligible. Assuming this channel is completely closed, the capillary force is the main driving force and the advancing direction is:

$$F = F_c - F_v \quad (1)$$

where F_c is the capillary force, F_v is the viscous force. Given

$$F_c = \gamma \cos \theta \cdot l_c \quad (2)$$

and

$$F_v = \frac{2l_c}{d_e} \eta x v \quad (3)$$

Thus there is:

$$F = \gamma \left(\cos \theta \cdot l_c - \frac{2l_c}{d_e} \eta x v \right) \quad (4)$$

where γ is the surface tension of water, θ is the water contact angle of nanofibrils, l_c is the perimeter of water column section (**Figure S12b**), d_e is the equivalent diameter of water column, η is the water viscosity, x is the transportation distance of water column and v is the water transportation velocity (**Figure S12c**).

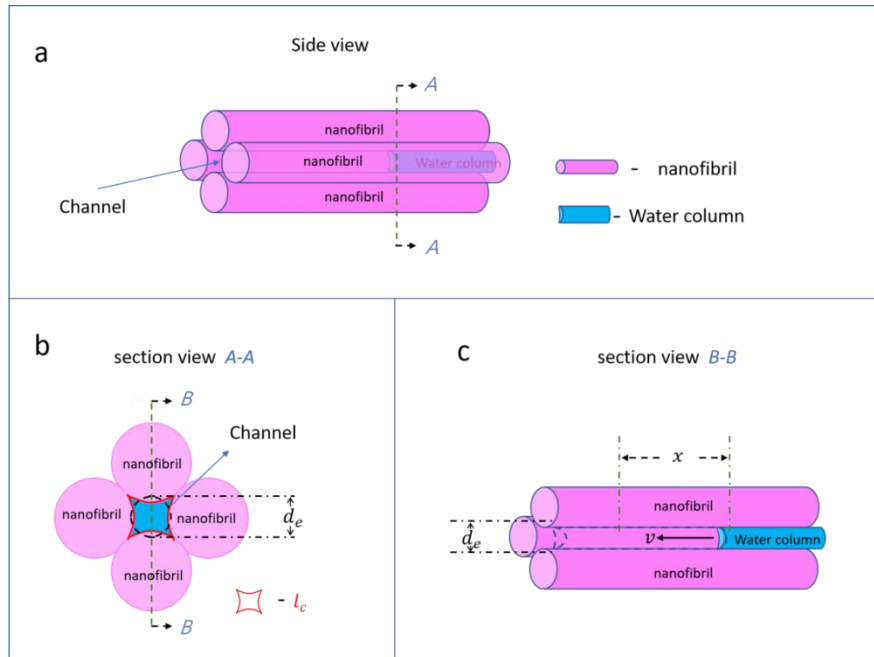


Figure S12. The main driving force in nanofibrils gaps of BNF from dry to semi-wetted state and the transport in wetted nano-fibric channel. a) The drawing show the side-view of four adjacent nanofibrils with water filled gap. The pink columns mark the nanofibrils. The blue dotted line marks the water. b) The drawing show the section view A-A of nanofibrils with water filled gap, as show in figure b. The red closed line marks the contact line between water and nanofibrils and l_c is the perimeter of water column section. The black chain dotted line marks the equivalent diameter of water column in nanofibrils gap. c) The drawing show the section view B-B of nanofibrils with water filled gap. The blue dotted line marks the transportation area of water column in the gap. The black arrow shows the transportation direction of water column, x is the transportation distance of water column and v is the water transportation velocity.

Supplementary analysis II:

The spindle-knot section is marked by the blue ellipse as shown in the middle section of **Figure S13**. The surface area of this blue ellipse (S_E) could be calculated by:

$$S_E = (4\pi/3)(2ab + a^2) \quad (1)$$

where a is equatorial radius and b is polar radius. The joint section is marked by the blue rectangle.

The surface area of joint section (S_J) could be calculated by:

$$S_J = 2\pi R(L_1 + L_2) \quad (2)$$

where R is the radius of joint, and L_1 and L_2 are lengths of joint sections on both sides of spindle-knot. The overlapping portions of the blue ellipse and blue rectangle is assumed as a spherical crown exhibited by a red dotted cycle. O is the center of this sphere and r is radius of this sphere.

The surface area of this spherical crown (S_C) could be calculated by:

$$S_C = 2\pi rH \quad (3)$$

where H is height of the spherical crown.

The height of the spherical crown (H) could be calculated by:

$$H = r - r\sin\beta \quad (4)$$

where β is the semi-apex-angle of hump.

The radius of the sphere (r) could be calculated by:

$$r = R/\cos\beta \quad (5)$$

The surface area of spindle-knot section (S_K) could be calculated by:

$$S_K = S_E - 2S_C = (4\pi/3)(2ab + a^2) - 2 \times 2\pi rH \quad (6)$$

Thus, the surface area of a BNF (S) could be calculated by:

$$S = S_K + S_J = S_E - 2S_C + S_J = (4\pi/3)(2ab + a^2) - 4\pi rH + 2\pi R(L_1 + L_2) \quad (7)$$

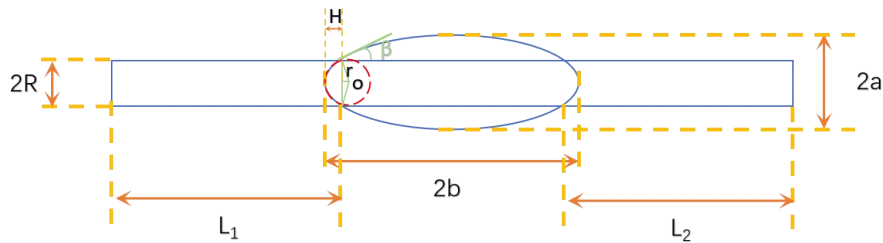


Figure S13. Sketch map of surface area calculation of a BNF.

Supplementary analysis III:

There are some common methods to calculate the critical volume of a droplet attached to an fiber. We used these methods calculated the critical volume of the droplet hanging on BNF and compared the results. The first method was deduced under absolutely ideal conditions, of which the droplet was assumed as a spherical on an even horizontal fiber (**Figure S14a**): ^[1]

$$\Omega \approx \frac{4\pi r \gamma \sin \beta}{\rho g} \quad (1)$$

Where β is the angle between horizontal and the line from the drop center to the three-phase point, r is the radius of the fiber. Because the BNF is not an even fiber with spindle-knot section and joint section, the critical volume was respectively calculated by this equation: $\Omega \approx 3.82 \mu\text{L}$ ($r = 50 \mu\text{m}$, the radius of joint), and $\Omega \approx 57 \mu\text{L}$ ($r = 75 \mu\text{m}$, the radius of spindle-knot). There are much difference between the results. Because the critical droplet was hanging mainly on the boundary of spindle-knot and joint, we think this result is not accurate. The real volume should be no larger than $57 \mu\text{L}$ and no less than $3.82 \mu\text{L}$. But only knowing a range is not enough. The second method was calculated from above equation on a spindle-knot fiber for two identical knots:

$$\Omega = \frac{2\gamma \cos \theta}{\rho g} (M + b\pi) \quad (2)$$

Where γ is the surface tension, θ is the contact angle of the water droplet on the BNF, ρ is density of water, g is the gravitational acceleration, M is the length of three phase line between the fiber and hanging water droplet, and b is the minor semi-axis of spindle knot.

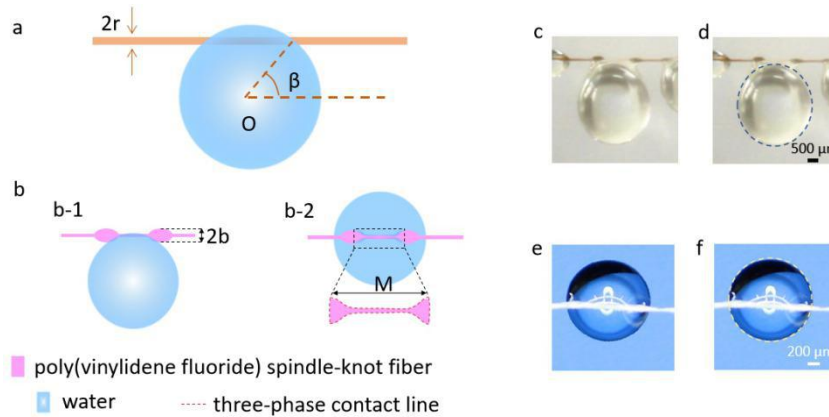


Figure S14. a) Illustration of fog collection on an even fiber. b) Illustration of fog collection on poly(vinylidene fluoride) spindle-knot fiber (b-1 is the side view; b-2 is the top view; pink and blue parts denote BNF and water drops, respectively, and red dashed line denotes the three-phase contact line). c) A droplet hang on BNF. d) Fitting the droplet with an blue dotted ellipse on the optical image. e) Top view of a small droplet hang on BNF. f) Fitting the small droplet with an yellow dotted circle on the optical image.

In this method, the three phase line was essential and supposed to be continuous because liquid film broke up along the fiber as shown in **Figure S14b**. In this cited article, this spindle-knot fiber was prepared by nylon fibers on which the collected water droplets were observed at clam-shell station. This shows that on this nylon fiber water droplet could not spread well. There was no stable water film covering this fiber during fog collection. So the author thought when hanging droplet was too large the part of droplet above nylon fiber could broke up entirely. Therefore, they believed the value of gravity of droplet was equal to the vertical component of the

product of water surface tension and length of three-phase contact line. But when the fiber is much more hydrophilic than nylon fiber and there is a stable water film on fiber during fog collecting, the water film would not break up easily or even not break up. This equation is not applicable any more. With a stable water film, when droplet detaching fiber, the water film is stretched. Because of the hump is an ellipsoid, its curved surface contact with water film with different angles. It is inaccurate to calculate the gravity of maximum hanging droplet using an apparent “contacting” angle. In theory, volume of maximum hanging droplet volume calculated through this “stretched water film method” should be larger than the result of “three-phase contact line method”, which means that the results of the “three-phase contact line method” is less than real value. Using the “three-phase contact line method” the critical droplet of BNF should be 4 μL . The volume of maximum hanging droplet (**Figure S14c**) was calculated through assuming it as an ellipsoid as shown in **Figure S14d**. We drew an ellipse on the optical image of maximum hanging droplet and found the most appropriate one to calculate the volume ignoring the rest. Our calculation result is 5.4 μL . This method is conservative and real because on BNF droplet was growing up symmetrical (**Figure S14e and f**) under the influence of water surface tension. Moreover, this method was chosen by above mentioned authors to verify their volume equation.^[2] So we believe this method is appropriate to give a real result.

[1] Pan, Z., Weyer, F., Pitt, W. G., Vandewalle, N., Truscott, T. T. Drop on a bent fibre[J]. *Soft Matter*, 2018, 14, 3724-3729.

[2] Hou, Y., Chen, Y., Xue, Y., Zheng, Y. & Jiang, L. Water collection behavior and hanging ability of bioinspired fiber[J]. *Langmuir*, 2012, 28, 4737-4743.

Supplementary Movies:

Movie S1: Water collection behavior of magnified BNF at fog flow rate of $20 \text{ g s}^{-1} \text{ m}^{-2}$.

Movie S2: Water collection behavior of BNF at fog flow rate of $150 \text{ g s}^{-1} \text{ m}^{-2}$.

Movie S3: Water collection behavior of BNF at fog flow rate of $65 \text{ g s}^{-1} \text{ m}^{-2}$.

Movie S4: Water collection behavior of BNF at fog flow rate of $20 \text{ g s}^{-1} \text{ m}^{-2}$.

Movie S5: Water collection behavior of BNF at low-temperature ($2 \text{ }^{\circ}\text{C}$) and fog flow rate of $65 \text{ g s}^{-1} \text{ m}^{-2}$.